PHYSICAL REVIEW B VOLUME 56, NUMBER 8 15 AUGUST 1997-II

Effective exciton mobility edge in narrow quantum wells

U. Jahn, M. Ramsteiner, R. Hey, and H. T. Grahn
Paul-Drude-Institut für Festkörperelektronik, Hausvogteiplatz 5-7, D-10117 Berlin, Germany

E. Runge and R. Zimmermann
Institut für Physik, Humboldt Universität zu Berlin, Hausvogteiplatz 5-7, D-10117 Berlin, Germany

(Received 2 July 1997)

An effective mobility edge for excitons in two-dimensional systems is shown to exist by comparing photoluminescence (PL) and PL excitation (PLE) with excitation-energy-dependent micro-PL spectra. The effective mobility edge of excitons shifts towards higher energies with increasing potential fluctuations. This blue shift is correlated with a sharp decrease of the PLE signal resulting in an extremely large energy separation between the PL and PLE spectra. Numerical simulations using a random potential confirm these results and predict a significant deviation of the PLE from the absorption spectrum. [S0163-1829(97)50636-9]

Electrons, holes, and their bound states (excitons) in semiconductor quantum wells (QW) can always be localized by random potential fluctuations at the interfaces due to their two-dimensional character. This is in strong contrast to electronic states in three-dimensional bulk material, where delocalized and localized states with infinite and finite localization length, respectively, are energetically separated by a sharp boundary, the so-called mobility edge.[1] Hegarty *et al.*[2] and Takagahara[3] have also applied the concept of a mobility edge to the relaxation behavior of excitons in 2D systems. This mobility edge E_m separates excitons with values of center-of-mass localization length on the order of the diffusion length from those with much smaller values. The former type of states is considered to be effectively delocalized, while the latter are localized. From a theoretical point of view,[3–5] localized states and the position of E_m are found in the low-energy part and near the center of the exciton absorption spectrum, respectively, which has been confirmed by several experiments.[2,6,7] So far, the experimental investigations have been focused on multiple QW structures predominantly with a rather large thickness of the QW, i.e., larger than 8 nm. These studies were based on time-resolved photoluminescence (PL) experiments such as frequency-domain four-wave mixing[2,6,8] and Rayleigh scattering,[2] as well as stimulated, picosecond photon-echo experiments[7] providing exciton relaxation rates or homogeneous linewidths as a function of the exciton energy E.

The recently developed method of μ-PL spectroscopy is ideal to investigate the effective exciton mobility edge in semiconductor QW's. The very sharp lines usually observed in μ-PL spectra at low temperatures originate from excitons localized at different potential minima with a depth determined by the respective size and shape.[9,10] In addition to ground-state excitons, these potential valleys can also contain optically active excited states.[10] Hence, μ-PL spectra can be used to image the landscape of the potential minima of the QW interfaces in a direct way. The upper part of the potential valleys should become visible when resonant excitation of higher states is achieved. A similar idea based on conventional PL spectroscopy was used to investigate E_m in bulk CdS_xSe_{1-x}.[11] The concept of an effective mobility edge in disordered QW's resembles to some respect the transport energy introduced for hopping processes in amorphous semiconductors.[12]

In this paper, we will demonstrate by experimental and theoretical considerations that the concept of an *effective* mobility edge E_m for the exciton motion in two-dimensional systems is applicable. The variation of the localization length as a function of energy in a QW with a certain type and structure of disorder is so rapid that E_m is quite well defined for a given temperature. In order to provide experimental evidence, we investigate μ-PL spectra of several narrow single QW's synthesized under well-defined, but different growth conditions. At the same time, all structures have been fully characterized by conventional PL measurements. The experimental results are supported by numerical simulations of the exciton energy relaxation in a random potential to obtain the corresponding PL, PL excitation (PLE), and absorption spectrum. Furthermore, for a random potential with a large amplitude, the effective mobility edge exhibits a shift towards the high-energy side of the exciton spectrum. This blue shift is correlated with a significant decrease of the intensity of the heavy hole (hh) PLE signal leading to an unusually high energy separation of the corresponding PL and PLE lines, which is often assigned to the so-called Stokes shift. We show that in the present case this assignment has to be corrected.

We have investigated three QW samples fabricated by molecular-beam epitaxy using different growth parameters, which are listed in Table I. Sample #1 has been grown under step flow conditions on a (001) GaAs substrate with a miscut angle of 2° towards (111)A. The growth conditions have been optimized for good optical quality, in particular for a small PL linewidth, but without showing any monolayer (ML) splitting of the PL line (Ref. 13 and references therein). Samples #2 and #3 are prepared on (001) GaAs substrates without any nominal miscut. In contrast to sample #1, the top and bottom barriers are formed by short period superlattices (SPSL) consisting of 11 and 50 periods, respectively, of 4 ML AlAs and 8 ML GaAs (1 ML corresponds to 0.283 nm). Using a SPSL for the bottom barrier avoids roughening of the bottom interface of the QW independently of the thick-

TABLE I. Growth conditions for the GaAs single QW's (samples #1–#3). T_G, BEP ratio, and SPSL denote the growth temperature, As_4-to-Ga beam equivalent pressure ratio, and short period AlAs/GaAs superlattice, respectively.

Sample	Substrate miscut	T_G (°C)	BEP ratio	Barrier	Well width (nm)	PL linewidth (meV)
#1	2° (111)A	605	16	$Al_{0.3}Ga_{0.7}As$	3.5	5.5
#2	0°	550	10	SPSL	4.8	9
#3	0°	610	30	SPSL	4.8	10

ness and the growth temperature (T_G) of this barrier. For the growth of sample #2, T_G was chosen to be below the usual temperature in order to induce a two-dimensional nucleation mode, whereas the higher As_4-to-Ga beam equivalent pressure (BEP) ratio used for sample #3 results in irregular and fuzzy growth steps.[14] Therefore, we expect rather rough top interfaces for samples #2 and #3. A first signature of the different random potentials induced by the different growth conditions are the increased PL linewidths of samples #2 and #3 compared to sample #1 (cf. Table I). All three samples have been investigated by PL, PLE, and μ-PL spectroscopy. The excitation was provided by a tunable Ti:sapphire laser pumped by an Ar^+ laser. The sample temperature was 5 K in the PL and PLE measurements and 8 K in the μ-PL experiments. The optical probe areas amounted to about 0.01 mm^2 in the PL and PLE and $1-2$ μm^2 in the μ-PL experiments.

Figure 1(a) shows the PL, PLE, and μ-PL results measured in sample #1. The data points (squares in the upper part) correspond to the *integrated* intensities $I(E_L)$ of the μ-PL spectra as a function of the respective laser energy E_L. Since only transitions below E_L can be detected (the laser line is suppressed by a notch filter), $I(E_L)$ depends not only on the absorption strength, but also on the exciton dynamics, which is also true for the PLE spectrum. $I(E_L)$ can be considered as an extended excitation spectrum, which is supported by the experimental observation that it essentially follows the conventional PLE signal. Therefore, the conclusions regarding the effective exciton mobility edge derived from the μ-PL spectra can be assumed to be representative for the respective sample. Since a direct measurement of the absorption in a single quantum well requires the removal of the substrate by chemical etching, the absorption and emission properties of this system can be changed, e.g., due to the induced strain. Therefore, we have estimated the expected absorption line (dotted line in upper part of Fig. 1) from a topographical model,[15] which predicts an almost Gaussian line shape with $S=0.553w$, where w denotes the width of the absorption line and S the Stokes shift. The value of w has been estimated from the light hole (lh) PLE linewidth. This procedure has been proven to be valid in a number of publications (cf. Ref. 15). We believe that our approach does not cause more uncertainties than does measuring the absorption spectrum after etching away the substrate.

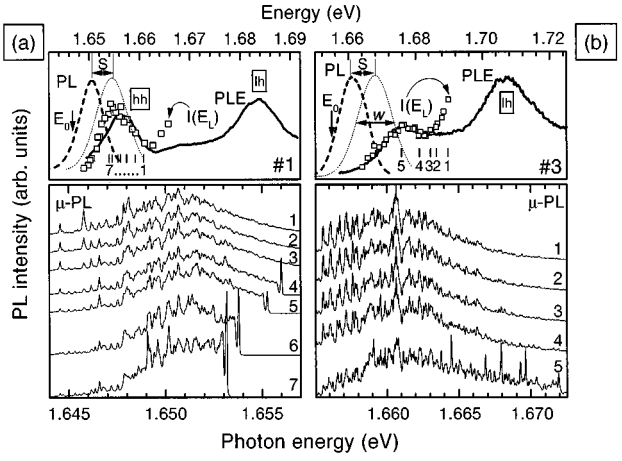

FIG. 1. PL (dashed line), PLE (solid line) detected at E_0, estimated absorption (dotted line), and normalized μ-PL spectra of sample #1 (a) and sample #3 (b). The open squares indicate the integrated intensities of the μ-PL spectra excited at the respective energies. The numbers in the upper part indicate the excitation energy of the μ-PL spectra in the lower part. The sample temperature in the PL and PLE measurements was 5 K, while the μ-PL spectra were recorded at 8 K.

Seven μ-PL spectra (1–7) recorded for different E_L are shown in the lower part of Fig. 1(a) with normalized intensities for a better comparison. The splitting into a large number of narrow lines indicates exciton localization due to random potential fluctuations, which are assumed to be due to thickness fluctuations as well as fluctuations of the barrier height.[13,16] With decreasing E_L beginning at the high-energy tail of the absorption line, the fine structure of the μ-PL spectra remains almost unchanged (spectra 1–5) until a critical energy is reached. Below this energy, some narrow lines exhibit an increase in intensity as observed in the spectra 6 and 7. Since the intensity of these lines decreases again for a further reduction of E_L (not shown here), their change in intensity is a result of a resonant excitation of higher exciton levels (center-of-mass eigenstates) localized within the same spatial region.

In Fig. 1(b), the PL, PLE, and some selected μ-PL spectra are shown for sample #3, which exhibits the largest potential fluctuations. Again, the fine structure of the μ-PL spectra remains unchanged with decreasing E_L down to a critical energy. However, compared to Fig. 1(a), this critical energy is shifted towards higher energies. A striking feature of the PLE spectrum in sample #3 is the much weaker signal of the hh line compared to sample #1, while the lh line seems to be of similar absorption strength in both samples. Hence, for QW's with large potential fluctuations, the hh PLE line cannot be used as a measure for the absorption strength anymore. Therefore, the absorption spectrum was again reconstructed using the model mentioned above.[15] Since for sample #1 this procedure provides an absorption line, which nearly agrees with the data of the excitation spectra [PLE and $I(E_L)$], we assume that the Gaussian line derived in this manner for sample #3 reflects its expected absorption spectrum. Furthermore, the energy difference between the esti-

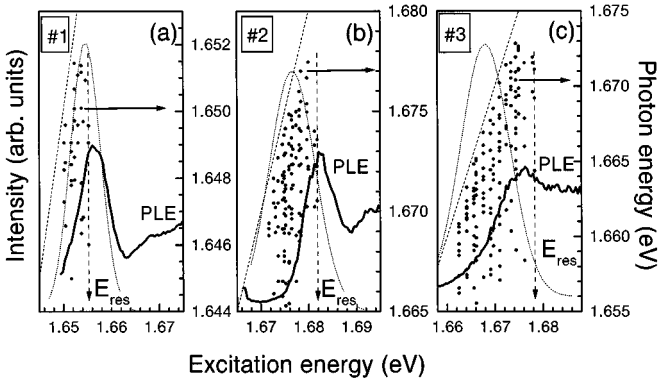

FIG. 2. PLE (solid line) and absorption spectra (dotted line) for all three samples under the same conditions as in Fig. 1. The data points indicate those μ-PL lines which are characterized by an increased intensity due to the resonant excitation of higher exciton states at the respective laser energy (short dashed line). The PLE spectra for samples #1 as well as #3 have been detected at E_0 (cf. Fig. 1) and for sample #2 at 1.664 eV.

mated hh absorption line and the measured lh PLE line agrees quite well with the calculated hh-lh splitting using the nominal parameters. The experimental data of sample #2 are similar to those of sample #3.

In order to determine the critical energy more accurately, the energetic position of all enhanced μ-PL lines has been evaluated as a function of the excitation energy. The results obtained for the three samples are shown in Fig. 2, where the estimated absorption line as well as the PLE spectra are also included. The energy E_{res} marked by arrows in Fig. 2 denotes the energy, below which resonant excitation into higher states occurs. The data for sample #1 in Fig. 2(a) clearly illustrate that resonant excitation of higher localized states is only detected for energies near or below the center of the absorption spectrum. In this respect, the μ-PL data of the state-of-the-art QW (sample #1) confirm earlier reported results for multiple QW's with thicker well widths and complement the time-resolved experiments of Refs. 2, 6, and 7. However, the results for samples #2 and #3 are very different. First, the energy E_{res} exhibits a remarkable shift to higher energies with increasing potential fluctuations, i.e., from sample #1 over #2 to sample #3. Second, this blue shift is correlated with a cutoff of the hh PLE signal, which leads to an almost complete suppression of the hh line in sample #3. If we interpret E_{res} as a measure for the position of the effective exciton mobility edge E_m, the blue shift of E_{res} cannot be explained using the concept discussed above,[3–5] because within this model the high-energy part of the exciton spectrum should be generally due to delocalized states. Nevertheless, the observed blue shift of E_{res} demonstrates the increasing importance of localized states going from sample #1 to sample #3, which is obviously responsible for the observed cutoff of the hh PLE spectrum. The fact that for samples #2 and #3 the shape and the width of the hh PLE lines do not agree with the ones of the respective lh lines clearly indicates a suppression of the hh signal on the low-energy side, which results in an increased deviation of the hh PLE spectrum from the actually expected absorption and therefore in a remarkable overestimation of the Stokes shift S. This conclusion is of particular importance for narrow QW's.

For a more detailed understanding of the exciton mobility edge, the relaxation kinetics of excitons in a QW have been studied numerically using quantum mechanical eigenstates of the exciton center-of-mass motion in a disordered potential. The relative motion of the electron and the hole is assumed to remain unchanged.[4] A kinetic equation is set up involving acoustic-phonon deformation-potential scattering, which dominates at low temperatures. The transition rates between states α and β, which have approximately the form

$$S_{\beta\leftarrow\alpha}=W(E_\beta-E_\alpha)\int d^2R|\Psi_\alpha(R)|^2|\Psi_\beta(R)|^2, \qquad (1)$$

depend strongly on the wave-function overlap in real space,[4] which is responsible for the selective filling of tail states observed in the μ-PL data. The temperature-dependent prefactor W distinguishes between phonon absorption and emission, and its magnitude determines the relative importance of relaxation compared to radiative emission $R_\alpha \propto|\int d^2R\Psi_\beta(R)|^2$. Once the eigenfunctions of a given realization of the disordered potential are known, the kinetic equation for the exciton occupation N_α

$$\frac{\partial N_\alpha}{\partial t}=G_\alpha+\sum_\beta S_{\beta\leftarrow\alpha}N_\beta-\left(R_\alpha+\sum_\beta S_{\beta\leftarrow\alpha}\right)N_\alpha \qquad (2)$$

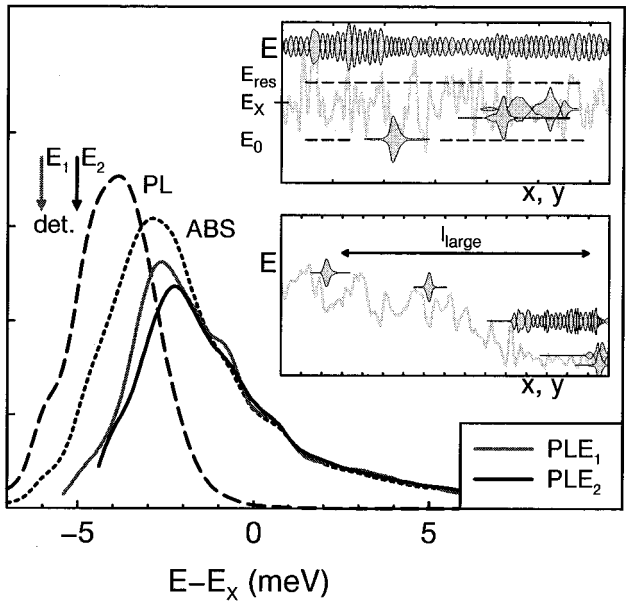

FIG. 3. Calculated PL (dashed line) and PLE spectra (solid lines) in comparison to the absorption ABS (dotted line) of a GaAs-$Al_{0.3}Ga_{0.7}As$ single QW with a thickness of 5 nm. The parameters used in the calculation are a potential variance of 8 meV caused by interface roughness, an exciton Bohr radius $R_B = 11$ nm, and a temperature of 5 K. The insets show schematically the potential fluctuations with and without a disorder component on a large length scale as well as typical wave functions at their respective energies. The upper part illustrates the type of disorder used in the numerical calculations.

including phonon scattering, absorption of the test pulse, and radiative emission, can be easily solved using a generation rate G_α and a data collection mode, which correspond to the particular experiment.

Figure 3 shows the results of the calculated absorption (ABS) and PL spectrum for a 5-nm-thick $GaAs/Al_{0.3}Ga_{0.7}As$ QW with interface roughness. The disorder conditions assumed in the calculations correspond to those of sample #1. The larger width of the PL and PLE lines found in the experiment are due to the narrower well width. The solid lines show two calculated PLE spectra for different detection energies. Calculations for different detection energies result in similar PLE spectra (solid lines) in agreement with experimental observations. The numerical results clearly exhibit an abrupt transition between rather extended states, which can relax into many different local minima, and rather localized states, which feed only very few local minima. This leads to a sharp decrease of the PLE efficiency, which is, within our accuracy, independent of the detection energy as observed experimentally. Note that for energies above this sharp decrease, which is identified as the effective mobility edge E_m, the PLE spectrum nicely follows the absorption. A shift of E_m towards the high-energy tail of the absorption spectrum, however, cannot be explained by the above theoretical consideration, where we have tacitly assumed that the energy fluctuations occur on a length scale of the exciton Bohr radius R_B or smaller (cf. upper inset of Fig. 3). In the opposite limit of very long-range fluctuations, the abrupt decrease in the PLE spectrum broadens, and E_m becomes spatially dependent. Therefore, as a route for the interpretation of the experimental results obtained in samples #2 and #3, we propose to take into account potential fluctuations on different length scales, since interface variations (roughness and/or alloy inhomogeneities) can consist of several components differing in the lateral correlation length.[17–20] Assuming that the inhomogeneous broadening of the exciton spectra in samples #2 and #3 is caused by a random potential with at least two significantly different lateral correlation lengths l_{small} and l_{large} (l_{small} is assumed to be on the order of R_B, while $l_{\text{large}} \gg R_B$), we can qualitatively explain both the blue shift of E_{res} and the suppression of the hh PLE line (cf. lower inset of Fig. 3). With decreasing laser energy, E_{res} is reached, when E_L enters the highest localized states of the large scale potential fluctuations. Since the density distribution of optically active excitons is determined by averaging over both kinds of fluctuations, E_{res} can appear on the high-energy side of the absorption line. For exciton energies below E_{res}, excitons cannot be transferred easily from the excited states in the high-energy regions to the detection states in the low-energy regions of the QW (cf. Fig. 3) giving rise to an increased suppression of the hh PLE signal.

In conclusion, for narrow QW's the effective mobility edge E_m can be well defined or inhomogeneously spread over the whole exciton spectrum depending on the growth-related amplitude and correlation length of the potential fluctuations. In the latter case the experimentally determined E_{res} is understood as the high-energy limit of the local E_m. For energies below this limit, states of the same energy may be localized within one part of the QW and delocalized within another. A proposed interpretation takes into account a random potential consisting of various components differing in the lateral correlation length. The suppression of the hh PLE signal due to disorder should generally be taken into account in the analysis of low-temperature PLE spectra.

Part of this work has been supported by the Deutsche Forschungsgemeinschaft within the framework of Sfb 296.

[1] E. Abrahams, P. W. Anderson, D. C. Licciardello, and T. V. Ramakrishnan, Phys. Rev. Lett. **42**, 673 (1979).
[2] J. Hegarty, L. Goldner, and M. D. Sturge, Phys. Rev. B **30**, 7346 (1984).
[3] T. Takagahara, Phys. Rev. B **32**, 7013 (1985).
[4] R. Zimmermann, F. Grosse, and E. Runge, Pure Appl. Chem. **69**, 1179 (1997).
[5] A. V. Kavokin, Phys. Rev. B **50**, 8000 (1994).
[6] H. Wang, M. Jiang, and D. G. Steel, Phys. Rev. Lett. **65**, 1255 (1990).
[7] M. D. Webb, S. T. Cundiff, and D. G. Steel, Phys. Rev. B **43**, 12 658 (1991).
[8] G. Bongiovanni, A. Mura, and J. L. Staehli, Superlattices Microstruct. **15**, 427 (1994).
[9] K. Brunner, G. Abstreiter, G. Böhm, G. Tränkle, and G. Weimann, Appl. Phys. Lett. **64**, 3320 (1994).
[10] D. Gammon, E. S. Snow, and D. S. Katzer, Appl. Phys. Lett. **67**, 2391 (1995).
[11] E. Cohen and M. D. Sturge, Phys. Rev. B **25**, 3828 (1982).
[12] D. Monroe, Phys. Rev. Lett. **54**, 146 (1985); S. D. Baranovskii, P. Thomas, and G. J. Adriaenssens, J. Non-Cryst. Solids **190**, 283 (1995).
[13] U. Jahn *et al.*, Phys. Rev. B **54**, 2733 (1996).
[14] R. Hey *et al.*, J. Cryst. Growth **175/176**, 1167 (1997).
[15] F. Yang, M. Wilkinson, E. J. Austin, and K. P. O'Donnell, Phys. Rev. Lett. **70**, 323 (1993).
[16] M. Ramsteiner *et al.*, Phys. Rev. B **55**, 5239 (1997).
[17] P. Ils, J. Kraus, G. Schaack, G. Weimann, and W. Schlapp, J. Appl. Phys. **70**, 5587 (1991).
[18] C. A. Warwick and R. F. Kopf, Appl. Phys. Lett. **60**, 386 (1992).
[19] R. Hey, M. Wassermeier, J. Behrend, L. Däweritz, K. Ploog, and H. Raidt, J. Cryst. Growth **154**, 1 (1995).
[20] K. Pond *et al.*, J. Vac. Sci. Technol. B **12**, 2689 (1994).